JCTC Journal of Chemical Theory and Computation

Article

pubs.acs.org/JCTC

On The Nature of the Halogen Bond

Changwei Wang,[†] David Danovich,[†] Yirong Mo,*[,‡] and Sason Shaik*[,†]

[†]Institute of Chemistry and The Lise Meitner-Minerva Center for Computational Quantum Chemistry, Hebrew University of Jerusalem, 91904 Jerusalem, Israel

[‡]Department of Chemistry, Western Michigan University, Kalamazoo, Michigan 49008, United States

Supporting Information

ABSTRACT: The wide-ranging applications of the halogen bond (X-bond), notably in self-assembling materials and medicinal chemistry, have placed this weak intermolecular interaction in a center of great deal of attention. There is a need to elucidate the physical nature of the halogen bond for better understanding of its similarity and differences vis-à-vis other weak intermolecular interactions, for example, hydrogen bond, as well as for developing improved force-fields to simulate nano- and biomaterials involving X-bonds. This understanding is the focus of the present study that combines the insights of a bottom-up approach based on ab initio valence bond (VB) theory and the block-localized wave function (BLW) theory that uses monomers to reconstruct the wave function of a complex. To this end and with an aim of unification, we studied the nature of X-bonds in 55 complexes using the combination of VB and BLW theories. Our conclusion is clear-cut; most of the X-bonds are held by charge transfer interactions (i.e., intermolecular hyperconjugation) as envisioned more than 60 years ago by Mulliken. This is consistent with the experimental and computational findings that X-bonds are more directional than H-bonds. Furthermore, the good linear correlation between charge transfer energies and total interaction energies partially accounts for the success of simple force fields in the simulation of large systems involving X-bonds.

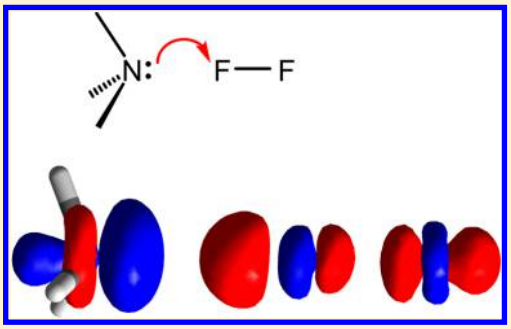

INTRODUCTION

The architecture and character of the macroscopic-, mesoscopic-, and nano-materials are fashioned by-and-large by relatively weak intermolecular interactions.[1−4] The interest of the chemistry community in various intermolecular interactions,[5] in the past decade or so, has been on a constant rise and has revealed the richness and nimbleness of these interactions and their high impact when they accumulate.[6]

One of these intermolecular interaction is the so-called halogen bond, or "X-bond", which is depicted on the top of Scheme 1 as Y:···X−Z. The X-bond involves an interaction of an electron rich center Y: of a Lewis base, with an electronegative halogen substituent X in an XZ molecule. The fascination with the X-bond and its renaming as such arise from the facts that (i) the interaction involves two electron rich centers, Y: and the electronegative halogen X, and (ii) the X-bond is highly directional and its YXZ angle is close to 180°, and as such, it constitutes an architectural element, much like the well-studied hydrogen bond (H-bond).[7−13]

Along with these roots of fascination, the interest in X-bonds has hugely surged because of the fact that this "bond" turns out to be ubiquitous in biological materials,[14,15] such as proteins, nucleic acids, and interactions of drugs with biological objects.[14] Thus, direct halogenation of proteins and nucleic acids, due to oxidative halogenation by peroxidases, generates artificial proteins and nucleotide bases. The latter even exhibit X-bond mediated base pairing, much like the H-bonds.[16] Thyroid hormones are naturally iodinated and utilize X-bonds of the Se:···I−I type as means of recognition and directing mechanisms.[17] A recent intriguing study[18] showed that the peptide-bond moiety of a protein can generate H- and X-bonds that are mutually perpendicular and can coexist without affecting the interaction energies and minimum distances of one another. Furthermore, X-bonds are essential architectural elements in supramolecular systems, liquid crystal engineering, nanomaterial design, nanowire formation, and so on and so forth.[11,19−21] These wide ranging applications have placed the X-bond in a center of great deal of attention. There is a need to understand the nature of the halogen bond, and this is the focus of the present study that combines the insights of a bottom-up approach based on valence bond (VB) theory,[22−25] and a hybrid approach based on block-localized wave function (BLW) theory.[26−29] To understand the roots of our approach and its motivation, we need to go back in time and prepare the background.

The history of X-bonds dates back to 1863 when Guthrie discovered the ammonia−iodine complex H_3N:···I−I.[30] During the 1940s the interest in similar donor−acceptor complexes was stimulated by spectroscopic measurements. These studies revealed the formations of 1:1 complexes between I_2 and benzene, and other dihalogens or halogenated compounds with solvents, which included O-donors, S-donors, or N-donors. As early as 1950, Mulliken formulated his charge-transfer (CT)

Received: May 15, 2014
Published: June 30, 2014

   dx.doi.org/10.1021/ct500422t | J. Chem. Theory Comput. 2014, 10, 3726−3737

Scheme 1. X-Bonds Studied in This Work[a]

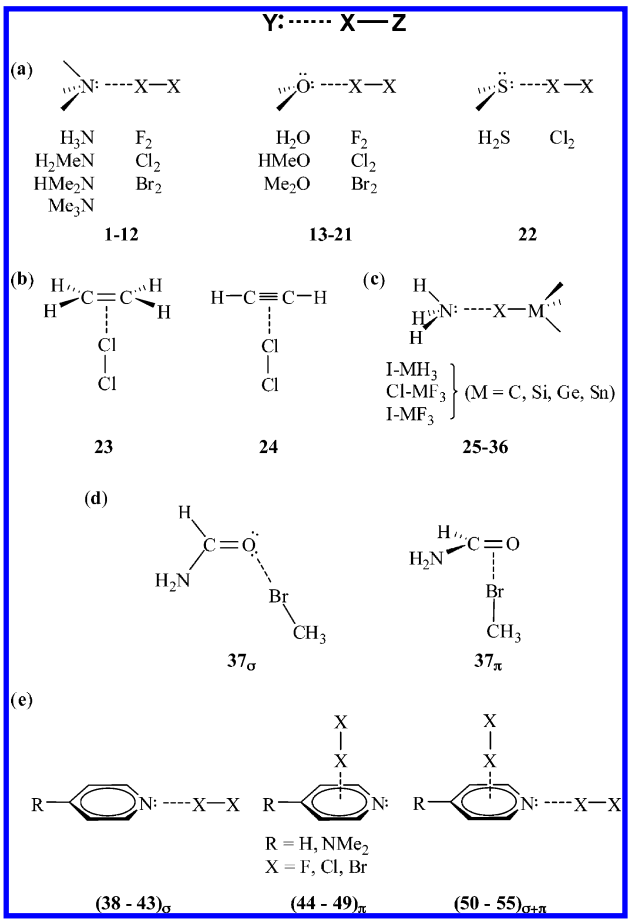

[a](a) complexes of Lewis bases with dihalogens, **17**−**22**, (b) complexes of simple π-systems with Cl_2, **23** and **24**, (c) complexes of ammonia with halomethanes and their heavy atom analogs, **25**−**36**, (d) π- vs. σ-complexes of carbonyl-containing molecules, with methyl bromide, $37_{\pi,\sigma}$, and (e) σ- vs π-complexes of substituted pyridines with dihalides, **38**−**55**.

theory, which has provided a framework for the understanding of the unique spectroscopy and dipole moments of these complexes in the ground- and excited states ever since.[31] His theory was in essence a valence bond theory that we use here, albeit in modern forms.

Many of these CT complexes were subsequently prepared by Hassel[32] who used X-ray and electron diffraction methods to reveal the beautiful structures of these "charge-transfer species", and to draw relations between the R_{YX} and R_{XZ} distances as indicators of the interaction in the Y:···X−Z complex.[32] The Mulliken CT theory has been used to describe these complexes until the interest in CT complexes, as such, faded. However, the field has never died out and was revived due to the above-discussed findings that this interaction of halogens with Lewis bases is a common motif in many materials and biosystems.[11,19−21] Dumas was the first to coin the term halogen bond (hence X-bond) for complexes of THF, pyridine, and anisole with tetrahalo-methane and silamethane.[33] This term gradually replaced the name CT complexes and is used today by the entire community.[2,12,34]

One of the most useful and pretty theoretical concepts for comprehending the intriguing features of the X-bond is the "σ-hole".[35−39] Politzer, Clark et al. showed that although halogen atoms carry partial negative charges, still the halogen has a region of positive electrostatic potential at the head of its lone pair and in the opposite direction of X−Z axis. This region is called "σ-hole", which can be understood as a crown of positive charge surrounded by a ring of negative charge along the extension of the X−Z bond.[35−39] Thus, the σ-hole confers electrostatic and polarization interactions, which account for the ability of the electronegative halogens to accept an interaction from electron rich centers, as well as for the linear YXZ angle.

The current discussions of experimental and theoretical studies of X-bonds are virtually dominated by the "σ-hole" notion and its electrostatic effects, some times to the exclusion of other effects. Thus, it is commonly argued that, at the limit of infinite basis set, polarization and CT are indistinguishable, and hence, any attribution of the stabilization energy X-bonds to CT interactions,[40,41] which lead to some Y···X covalence is perhaps no more than an artifact,[35] (see, though, ref 42). However, as was shown by Alvarez,[4] many of the intermolecular interactions tend to exhibit continuum of distances and hence presumably also of energy contributions. Therefore, a monolithic approach that is based exclusively on the electrostatic origins may be missing an essential feature of the X-bond.[43] Moreover, polarization (POL) and CT have distinctly different physical origins; POL originates in electron excitations within the constituents of the complex, while CT arises from electron excitation between the constituents. Since the two constituents are distinguishable by experiment, then POL and CT are distinctive physical phenomena, and the infinite basis set argument artificially misses the chemical distinguishability. There may well be X-bonds that are dominated by electrostatics (ES) and polarization (POL), others by dispersion (DISP), and still others by CT. For sure, the symmetric trihalides X_3^-, which are extreme cases of X-bonding, where the Lewis base is $X:^-$, must involve significant CT interaction.[34,40,44−46] Thus, with an aim of unification, we studied here the nature of the X-bonds enumerated in Scheme 1 using the combination of VB and BLW theories.[25−27] As we shall demonstrate, with the exception of weak X-bonds, the great majority of the complexes are bonded by CT interactions as envisioned by Mulliken more than six decades ago. We note that, in a recent work, Grabowski performed NBO computations, and argued that halogen and hydrogen bonds are both ruled by the same hyperconjugation, that is, charge transfer, and rehybridization effects.[47] Due to the very different natures of the NBO method, where localized orbitals are derived by a series of post-SCF transformations, and the VB/BLW method, where localized orbitals are self-consistently optimized, it is essential to re-examine the mechanism of halogen bonds, as VB/BLW studies showed that the hydrogen bonds are usually dominated by the electrostatic interaction, though the charge transfer (hyperconjugation) effect plays a non-negligible role.[48]

The complexes in Scheme 1 are subdivided into five categories. In Scheme 1a, we studies X-bonds (**1**−**22**) between amines, water, methanol, ether, and H_2S with three dihalide molecules. These kinds of X-bonds contain the originally discovered CT complexes and/or their simplified models (e.g., Me_2O:···BrBr models the Hassel complex of dioxane with Br_2).[11,30,32] Our calculations further verify that the magnitude of σ-holes in dihalogens increases in the order of $F_2 < Cl_2 < Br_2$ (see Supporting Information (SI)).

dx.doi.org/10.1021/ct500422t | J. Chem. Theory Comput. 2014, 10, 3726−3737

Scheme 1b shows two complexes (**23** and **24**), which belong to the classical π−CT complexes,[31] and have also been invoked as intermediates in electrophilic substitution reactions. Scheme 1c describes models of the classical CT complexes formed between amines and various haloform molecules (**25**−**36**), which have been studied by Hassel,[32] Dumas,[33] and recently by means of MP2 computations.[43] As halogen bonds are involved in substrate−protein interactions where the main chain or side chain structure of protein residues can be mimicked by formamide, Scheme 1d shows cases with a "peptide bond" ($\mathbf{37}_{\pi,\sigma}$) where the Br-bond can take presumably two different positions vis-à-vis the C═O moiety, one as a π-complex, the other as a σ-complex. The selectivity is interesting in view of the recent results of Voth et al.,[18] that a model of the peptide moiety enables the coformation of H- and X-bonds, which are mutually perpendicular. Finally, the systems in Scheme 1e ($(\mathbf{38}-\mathbf{55})_{\pi,\sigma}$) further probe the question of selectivity of the X-bonds with potentially ambident Lewis bases. Thus, while pyridine has a lower N-lone pair ionization potential, the dimethylamino substituted pyridine has a lower π-ionization potential.[49] Will the pyridine substituent (R = NMe_2) create a preference for π-complex formation, or will the CT energy favor the more localized interaction via the N atom of the pyridine moiety?

The above complexes were studied using the combination of VB and BLW theories. VB theory, which is a bottom-up approach, defines the energetic contribution of POL and CT using chemically lucid wave functions. The BLW method, which is a hybrid of VB and MO theories, defines the total wave function/electron density by limiting the expansion of each orbital within one interacting fragment (monomer), thereby allowing consideration of CT and POL separately. The presently employed BLW energy decomposition method is related to the general class of energy decomposition analysis (EDA) methods.[50−60] However, the BLW method itself is unique as it is NOT an analysis of an SCF (Self-Consistent Field) wave function, rather, it derives self-consistently the electron-localized state wave function. All these top-down EDA methods including the NBO-based ones[46,54] reflect the recognition that the application of a local approach to analyze weak intermolecular complexes of the X-bond type is ultimately productive and insightful.[61]

Theoretical Strategy. Figure 1 schematizes the essentials of the VB and BLW approaches for describing the bonding contributions to the generic Y:···X−X complex.

The VB wave function is given as a linear combination of the VB structures in Figure 1a. This VB-set includes all the possible modes of distributing the four active electrons, the lone pair of the base Y: and the bond pair of X−X, in the valence of the Y and X_2 fragments. The first three configurations are the covalent (Φ_{cov}) and ionic structures (Φ_{ion}/Φ'_{ion}) that together describe the X−X bond in the presence of the Y: base. Two of the remaining three structures belong to a charge transferred state (Φ_{CT}), wherein an electron from Y: is transferred to the X−X moiety, resulting in one structure in which the odd electrons are singlet paired to form a short Y·—·X_1 bond, and the second structure having a long bond Y·—·X_2 separated by an anion X:$^-$ in the middle (i.e., a singlet diradical with two odd electrons weakly coupled).[44,62] Finally, the sixth structure is di-ionic involving two electron transfer to the X-X moiety. This structure, which formally belongs to Φ_{CT} too, is very high in energy and its contribution is rather negligible.

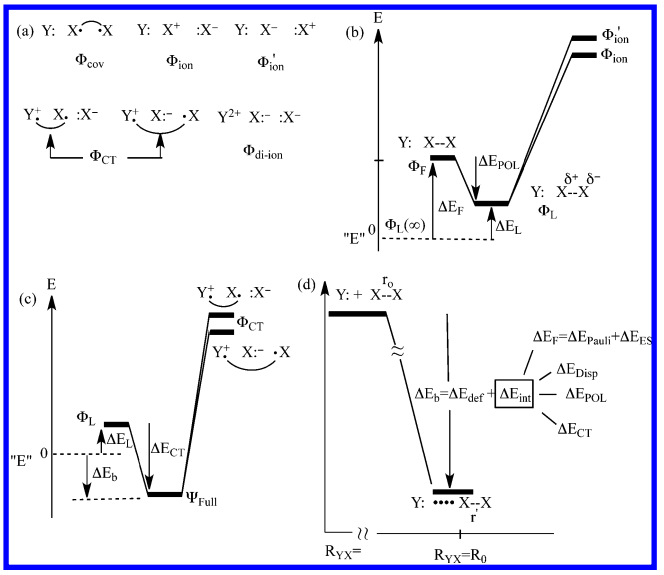

Figure 1. (a) VB structure set required for the description of the Y:··· X−X. (b, c) VB mixing diagrams showing the key energy terms responsible for the X-bonding, by means of polarization (POL) in part b, and by means of CT in part c. Part b defines also the repulsive energy (ΔE_F), in the frozen Lewis state, Φ_F, and the stabilizing polarization energy (ΔE_{POL}), when the Lewis state relaxes by remixing of its ionic structures to allow for polarization in the Y: ($X^{\delta+}$−$X^{\delta-}$) sense. Part c shows the mixing of the Lewis state with the VB components of the CT state to obtain the final state of the X-bond (Ψ_{full}), which is stabilized thereby by the CT energy, ΔE_{CT}. The bonding energy of the X-bond ΔE_b, is a balance between the stabilizing charge transfer energy and the residual repulsion in the relaxed Lewis state, $\Delta E_b = \Delta E_{CT} - \Delta E_L$. (d) The BLW dissection of the binding energy ΔE_b of the X-bond. The initial decomposition provides the interaction energy (ΔE_{int}) by calculating the deformation energy of the molecules, ΔE_{def}, and finding $\Delta E_{int} = \Delta E_b - \Delta E_{def}$. Subsequently, ΔE_{int} is further decomposed into various terms, as shown in the Figure.

To obtain good energies, we use the breathing orbital VB (BOVB) approach,[63,64] which includes dynamic correlation in the VB structures and the VB mixing (see Methods). All the VB calculations show that the di-ionic structure is unimportant, and hence, it will not be mentioned anymore. The VB method enables us to define the various contributions due to the X-bond formation, as schematized in Figure 1b and c using VB mixing diagrams.[65−67]

Thus, as shown in Figure 1b, if we just use the first three covalent and ionic structures, we are going to derive the state Y: (X−X), which describes the base and the X_2 molecule with a Lewis bond, hence the Lewis state. If we calculate this state at a very long distance (e.g., 27 Å where energy converges) where there is no intermolecular interaction, the so obtained wave function simply describes a nonbonded state labeled in Figure 1b as $\Phi_L(\infty)$. Note that, as X_2 is described with one covalent and two ionic structures, $\Phi_L(\infty)$ is composed of Φ_{cov}, Φ_{ion}, and Φ'_{ion} (Figure 1a). If we bring Y and X_2 to the optimum geometry of the X-bond without allowing any change in the Lewis wave function, we obtain the frozen nonbonded state, Φ_F, whose energy will rise due to Pauli repulsion (ΔE_{Pauli}) and the deformation energy of the fragments (ΔE_{def}) and be stabilized by the electrostatic interaction between the moieties (ΔE_{ES}). The net energy change of the frozen Lewis state is ΔE_F in Figure 1b, and our VB calculations show that this quantity is

dx.doi.org/10.1021/ct500422t | J. Chem. Theory Comput. 2014, 10, 3726−3737

Table 1. Halogen Bond Distances (Å) and BLW Energy Contributions to the Binding Energies (kcal mol^{-1}) in Halogen Bonding Complexes (Y:···X−X, 1−24) at the ωB97x-D/cc-pVTZ Theoretical Level Compared with VB Values in Parentheses

complex	R_{YX}[a]	R_{XX}	ΔE_{def}	ΔE_F	ΔE_{Disp}	ΔE_{POL}	ΔE_{CT}	ΔE_{int}	ΔE_b
1−12									
$H_3N\cdots F_2$	2.5145	1.3990	0.23	2.10 (1.84)	−0.41	−0.39 (−0.69)	−2.99 (−2.01)	−1.68	−1.45 (−0.86)
$H_2MeN\cdots F_2$	2.3223	1.4273	1.24	5.63	−0.70	−0.62	−7.79	−3.48	−2.24
$HMe_2N\cdots F_2$	2.0624	1.5113	7.32	17.81	−1.04	−1.51	−26.02	−10.76	−3.44
$Me_3N\cdots F_2$	1.9146	1.5943	16.22	32.94 (34.75)	−1.37	−2.97 (−3.23)	−49.81 (−35.55)	−21.22	−4.99 (−4.03)
$H_3N\cdots Cl_2$	2.6175	2.0326	0.34	2.55 (2.78)	−0.50	−1.50 (−1.75)	−6.08 (−6.48)	−5.53	−5.18 (−5.45)
$H_2MeN\cdots Cl_2$	2.5299	2.0475	0.70	5.05	−0.82	−2.04	−9.40	−7.20	−6.50
$HMe_2N\cdots Cl_2$	2.4559	2.0627	1.15	8.20	−1.15	−2.73	−13.01	−8.69	−7.54
$Me_3N\cdots Cl_2$	2.4222	2.0714	1.46	10.26 (10.89)	−1.50	−3.27 (−3.59)	−15.13 (−17.69)	−9.63	−8.17 (−10.39)
$H_3N\cdots Br_2$	2.6507	2.3244	0.41	2.57	−0.60	−2.36	−7.09	−7.49	−7.08
$H_2MeN\cdots Br_2$	2.5714	2.3397	0.74	5.14	−0.99	−3.23	−10.40	−9.47	−8.73
$HMe_2N\cdots Br_2$	2.5136	2.3534	1.11	7.93	−1.39	−4.19	−13.40	−11.04	−9.93
$Me_3N\cdots Br_2$	2.5024	2.3575	1.26	9.12	−1.83	−4.61	−14.45	−11.77	−10.51
13−21									
$H_2O\cdots F_2$	2.7167	1.3824	0.00	0.56	−0.36	−0.07	−0.69	−0.57	−0.57
$HMeO\cdots F_2$	2.6570	1.3836	0.00	0.66	−0.56	−0.10	−0.84	−0.84	−0.84
$Me_2O\cdots F_2$	2.6397	1.3835	0.00	0.77	−0.80	−0.11	−0.87	−1.01	−1.01
$H_2O\cdots Cl_2$	2.7595	2.0089	0.02	0.17 (0.41)	−0.37	−0.53 (−0.60)	−1.91 (−3.05)	−2.64	−2.62 (−3.23)
$HMeO\cdots Cl_2$	2.7030	2.0112	0.06	0.62	−0.66	−0.66	−2.48	−3.18	−3.11
$Me_2O\cdots Cl_2$	2.6848	2.0117	0.07	0.93	−0.97	−0.72	−2.73	−3.49	−3.42
$H_2O\cdots Br_2$	2.7951	2.2953	0.03	−0.09	−0.43	−0.84	−2.32	−3.68	−3.65
$HMeO\cdots Br_2$	2.7461	2.2981	0.09	0.38	−0.81	−1.04	−2.97	−4.45	−4.36
$Me_2O\cdots Br_2$	2.7113	2.2995	0.14	0.93	−1.19	−1.19	−3.37	−4.82	−4.68
22									
$H_2S\cdots Cl_2$	3.2077	2.0113	0.02	1.16	−0.37	−0.31	−2.61	−2.13	−2.11
23−24									
$H_2C{=}CH_2\cdots Cl_2$	3.1064[b]	2.0084	0.02	1.02	−0.75	−0.30	−2.11	−2.13	−2.11
$HC{\equiv}CH\cdots Cl_2$	3.1882	2.0044	0.01	0.38	−0.53	−0.21	−1.32	−1.67	−1.67

[a]Y = N, O, and S. [b]R(Y···X) of $ClCl\cdots C_2H_4$ is the distance of the Cl atom to the middle of the C=C bond.

positive, namely, the attractive electrostatic interaction cannot offset the Pauli repulsion in the frozen Lewis state.

In the next step, the Lewis state is allowed to relax its electronic structure by self-consistently adjusting the contributions of its two ionic configurations, Φ_{ion} and Φ'_{ion}, to the presence of the Y: base. The result is that Φ_{ion} which places X^+ adjacent to the negative potential of the Y: becomes more important. The bond gets polarized, and we obtain the relaxed Lewis state, Φ_L. The energy change is the polarization energy ΔE_{POL} that stabilizes the Lewis state. As seen in Figure 1c, the result of all the computations is that Φ_L still lies above the no-bond state $\Phi_L(\infty)$ by ΔE_L. Hence, the combined electrostatic and polarization interactions cannot overcome the Pauli repulsion and drive the formation of an X-bond!

Finally, in Figure 1c, we show the mixing of the relaxed Lewis state with the two structures of the CT state. In the presence of $Y^{\cdot+}$, these structures have different energies; the one placing the $X:^-$ adjacent to $Y^{\cdot+}$ is stabilized relative to the other. The $\Phi_L-\Phi_{CT}$ mixing, gives rise to the X-bond, due to the charge-transfer stabilization energy ΔE_{CT}. If $|\Delta E_{CT}| > \Delta E_L$, a stable X-bond will be formed. Our calculations show that this is the case for all the complexes studied with VB theory.

Let us now turn to Figure 1d to inspect the BLW perspective of the X-bond. The analysis is customarily applied in DFT. The steps of the energy decomposition were recently described in great detail,[26,27] and only a brief summary follows. The method calculates first the binding energy ΔE_b, as a difference between the X-bonded state and the no-bonded state (composed of separated molecules). Since the individual molecules in the X-bond complex have geometries different from the relaxed molecules, one can calculate the deformation energy ΔE_{def} of the molecules, which is the energy required to distort the molecules into their geometry in the complex.[50,51,60,68−71] Given ΔE_b and ΔE_{def}, one can obtain the total interaction energy ΔE_{int} between the fragment as the difference, $\Delta E_{int} = \Delta E_b - \Delta E_{def}$. The latter quantity is then decomposed further to the various energy terms shown by the lines emanating from the boxed ΔE_{int} in Figure 1d.

Thus, a regular self-consistent field calculation on the Y:···X−X complex while retaining all electrons in their respective monomers, but including all mutual electron−electron interactions and electron−nuclear attraction terms, gives rise to the BLW state where there is no electron delocalization between Y: and X−X. The CT term, ΔE_{CT} (further corrected for BSSE), is then obtained as the difference between the energies of the X-bond complex and the corresponding BLW (electron-localized) state. The credibility of the procedure has been amply demonstrated in the studies of conjugated systems where computational results, including geometric, spectral, and energetic, are consistent with viable experimental information.

In the BLW state, the distorted molecules are themselves electronically relaxed, and thus, as the two distorted molecules are brought to the geometry of the complex but are not allowed to relax electronically, one obtains the initial BLW0 state. Taking the energy difference E(BLW)-E(BLW0), we obtain the polarization contribution to bonding, ΔE_{POL}. Bringing the assembly of the deformed molecules into the geometry of the

dx.doi.org/10.1021/ct500422t | J. Chem. Theory Comput. 2014, 10, 3726−3737

complex without allowing them to relax electronically, provides the steric energy, ΔE_S, which is a sum of the Pauli, electrostatic and long-range dispersion energies, $\Delta E_S = \Delta E_{Pauli} + \Delta E_{ES} + \Delta E_{Disp}$ (hence, $\Delta E_S = \Delta E_F + \Delta E_{Disp}$). However, we usually list ΔE_{Disp} as a separate energy term. The separate calculation of the dispersion provides the quantity $\Delta E_F = \Delta E_{Pauli} + \Delta E_{ES}$, which is analogous to the destabilization energy of the frozen Lewis state, accessible from VB (see Figure 1b).

Importantly, *in order to rule out the overestimation of CT energy* the BLW method employs here DFT with the range-separated functional ωB97x-D/cc-pVTZ.[72] The VB method we use is BOVB, which is an ab initio VB method that incorporates dynamic correlation.[63,64] In this manner, we describe the X-bonded complexes by two methods that are entirely different albeit having a clear affinity. Let us see the outcome of the modeling.

RESULTS AND DISCUSSION

Comparison of BLW and VB Results. Geometries were optimized at the ωB97x-D/cc-pVTZ level of theory, and the key bond distances are listed in Table 1 and SI Table S1. Notably, the X−X molecule approaches the lone pair on the nitrogen atom of $Me_nH_{3-n}N$ and the oxygen atom of $Me_nH_{2-n}O$, or the center of the π bond in ethylene or acetylene. Compared with the monomer halogen gas, the X−X bond distance stretches and this elongation increases with the gradual substitution of hydrogen atoms by methyl groups in $Me_nH_{3-n}N$ and in $Me_nH_{2-n}O$. The largest elongation is observed in the $Me_3N\cdots F_2$ complex where the F−F bond stretches by 0.2174 Å. For comparison, the X−X bond varies only 0.0740 Å in $Me_3N\cdots Cl_2$ and 0.0767 Å in $Me_3N\cdots Br_2$.

Table 1 summarizes the results of the BLW and VB calculations for the X-bonds **1**−**24**, where the ΔE_{Disp} term equals to the Grimme's dispersion correction of the complex by reference to the sum of the dispersion energies within monomers at the complex geometry.[73] Figures 2−4 provide some essential trends from the computed data. The geometric details for the complexes, results of calculations of σ-holes, and electron density analyses are relegated to the SI.

Inspection of the data in Table 1 reveals that both BLW and VB arrive at the same conclusions with respect to the total binding energies, ΔE_b, and its key components. In all the common complexes studied in this work, the steric energies (which can be generally defined as the sum of ΔE_F and the dispersion effect ΔE_{Disp}) are positive for **1**−**12** and close to zero for **13**−**24**, and the polarization energy is negative (stabilizing) but small, indicating that the stabilizing electrostatic and polarization energies are too small to overcome the Pauli repulsion, while the CT energy ΔE_{CT} overwhelmingly dominates the binding, Thus, *these X-bonds do not originate in electrostatics or polarization but are driven by the CT interaction*.

Figure 2 shows these conclusions in terms of correlations between the VB and BLW quantities. Specifically, Figure 2a reveals that the total binding energies, ΔE_b, of the common X-bond complexes correlate quite well for the two methods, and even the absolute values are not too far from each other, which is remarkable considering the very different computational approaches. Figure 2b shows the correlation for the dominant term, the CT interaction energy ΔE_{CT}. The correlation is good and the absolute magnitudes of the values are close. Figure 2c, shows a good correlation for the polarization component ΔE_{POL}. Both methods show that the Lewis state undergoes polarization in the Y: ($X^{\delta+}$—$X^{\delta-}$) sense. In Figure 2d, VB

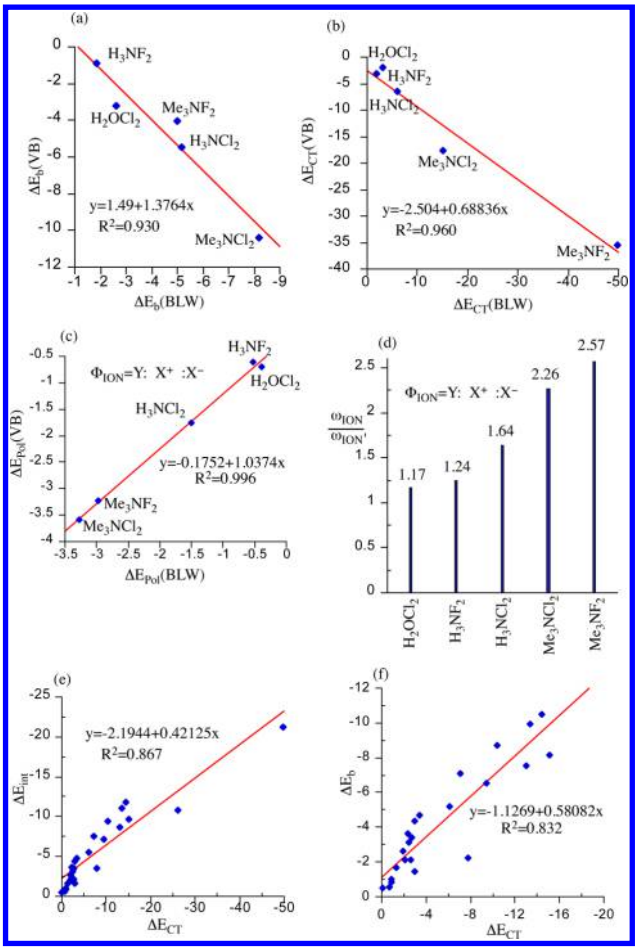

Figure 2. Correlations of VB and BLW results for common Y:···X−X complexes: (a) ΔE_b(VB) vs ΔE_b(BLW). (b) ΔE_{CT}(VB) vs ΔE_{CT}(BLW). (c) ΔE_{POL}(VB) vs ΔE_{POL}(BLW). (d) Ratio of the weighs of Φ_{ion} and $\Phi_{ion'}$ in the Lewis state Φ_L. Correlations of BLW calculated ΔE_{CT} with (e) ΔE_{int} and (f) ΔE_b. All energetic terms are in kcal mol^{-1}.

theory shows explicitly the mechanism of this polarization in terms of the relative weights of the two ionic structures, Φ_{ion} to Φ'_{ion}. It is seen that this ratio varies between 1.167 for the most weakly polarized case, $H_2O\cdots Cl-Cl$, to ∼2.57 for the most polarized cases e.g., $Me_3N\cdots F-F$. The same conclusion was derived from the BLW results for the Lewis state, as exemplified by the electron density difference (EDD) maps, which exhibit the redistribution of the electron density within each monomer due to the influence of the other, for the five systems explored by VB theory in Figure 3, where blue color represents a loss and the red refers to a gain of electron density. With the approach of the Lewis base, the electron density in X_2 unanimously moves away from the Lewis base, resulting in the Y: ($X^{\delta+}$—$X^{\delta-}$) type of polarization as verified by VB computations. Numerical population analyses based on the NBO method (as presented in SI, Table S5) further endorse this finding.

Trends in the BLW Results for 1−24. Parts e and f of Figure 2 display the extensive BLW trends. Figure 2e shows that the total interaction energy ΔE_{int}, correlates generally with the CT energy term, ΔE_{CT}. Since the deformation energies, ΔE_{def}, are very small for most of the cases (Table 1), with the exception of $Me_3N\cdots F-F$ and $Me_2HN\cdots F-F$, if these two outliers are removed, the ΔE_{int} and hence also ΔE_{CT} correlate

dx.doi.org/10.1021/ct500422t | J. Chem. Theory Comput. 2014, 10, 3726−3737

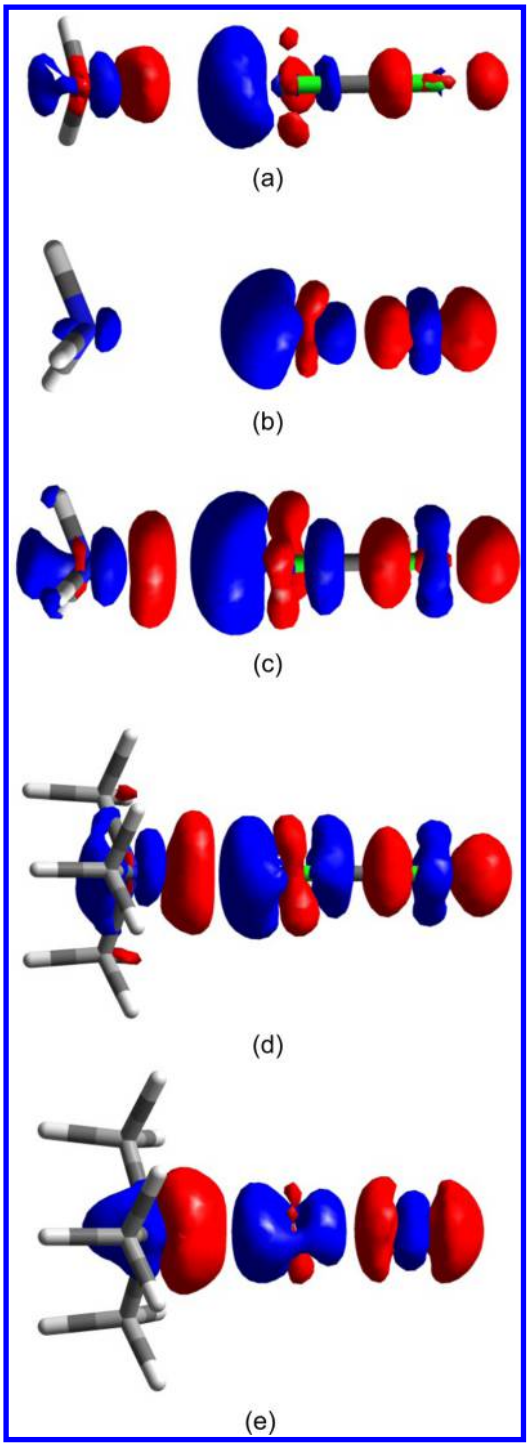

Figure 3. Electron density difference (EDD) maps showing the polarization in the Lewis states of (a) $H_2O\cdots Cl_2$; (b) $H_3N\cdots F_2$; (c) $H_3N\cdots Cl_2$; (d) $Me_3N\cdots Cl_2$; (e) $Me_3N\cdots F_2$. The isodensity value is 0.001 au.

generally with the binding energy, ΔE_b. Figure 2f shows the $\Delta E_{CT}/\Delta E_b$ correlation (see also Table 1). Thus, the CT energy term emerges as a key driving force for most of the X-bond complexes in Table 1. The correlation between ΔE_{int} and ΔE_{CT} has a far-reaching significance in the development of force fields as there is no particular term for the electron transfer interactions yet. Similar ΔE_{int} versus ΔE_{POL} correlation was identified in the previous study of the δ-opioid receptor−ligand bindings.[74] These approximate linear correlations indicate that both polarization and charge transfer interactions can be effectively absorbed (or more precisely, have been absorbed without realization) into the electrostatic energy term by adjusting the relevant parameters (mostly the partial atomic charges) in the parametrization process of force fields. This explains the remarkable success of force fields in the simulation of systems concerning halogen bonds (and π-cation interactions), though there are current endeavors to develop next-generation forces fields, which contain explicit terms for the polarization effect.

CT Energies of X-Bonds 1−24. The factors that govern the CT energy term are the energy gap in Figure 1c, and the coupling matrix element between the Lewis state and the CT state. At infinite intermolecular separation, the energy gap for the CT state is given by the difference of the ionization potential $IP_{Y:}$ of the base and the electron affinity EA_{XX} of the dihalogen molecule. Table 2 compiles the values of adiabatic IP and EA. Our limited VB-data set show these expected dependencies. The more extensive BLW data further support these trends in a rather compelling manner.

Table 2. Computed Adiabatic Ionization Potential (IP) of Lewis Bases and Electron Affinity (EA) of Dihalogens at the ωB97x-D/cc-pVTZ Theoretical Level Compared with Experimental Data[a]

base	IP	IP (exptl)	X_2	EA	EA (exptl)
H_3N	10.130	10.02	Br_2	2.572	2.42002
H_2MeN	8.947	8.9	Cl_2	2.427	2.33004
HMe_2N	8.203	8.2 ± 0.1	F_2	2.785	3.07998
Me_3N	7.724	7.8			
H_2O	12.539	12.65 ± 0.05			
HMeO	10.720	10.85 ± 0.03			
Me_2O	9.802	10.025 ± 0.025			

[a]NIST Standard Reference Database Number 69 (http://webbook.nist.gov/chemistry/). All IP and EA data are in eV units.

Since we have only three dihalogen molecules and twice as many bases, the correlation with $IP_{Y:}$ is more impressive and is shown in Figure 4a. It is seen that the range of ΔE_{CT} values diminishes as the $IP_{Y:}$ increases from the low value for Me_3N to the high value for H_2O. This type of correlation was amply observed experimentally.[11] Note that the range of ΔE_{CT} for Me_3N and Me_2HN is very large, reflecting the fact that with the stronger bases, Me_3N and Me_2HN, interacting with F_2, there is a considerable F−F bond cleavage and the N···F distance is rather short. Thus, these complexes are already advanced along the nucleophilic-displacement trajectory to yield, for example, M_3NF^+ F^-.[44,45,62] This can be verified by the in situ HOMO−LUMO gap,[75] which refers to the orbital energy difference when both interacting molecules are put together with no orbital-mixing (electron transfer) occurring yet, for the series of $Me_nH_{3-n}N\cdots F_2$ (n = 0−3), which are 0.324, 0.274, 0.205, and 0.156 eV with n increasing from 0 to 3. Indeed, as noted by Legon, some of the X-bonds with dihalogens are unstable to such nucleophilic-displacement decomposition.[11]

Using simple perturbation theory, the weight of the CT state mixing into the Lewis state (Figure 1c) is the amount of charge transferred, Q_{CT}, from the Lewis base to the X_2 molecule. Figure 4b shows indeed the existence of an excellent linear correlation between ΔE_{CT} and Q_{CT}. Since the binding and interaction energies correlate generally with ΔE_{CT} we expect to find also a general $\Delta E_{int}/Q_{CT}$ and $\Delta E_b/Q_{CT}$ correlation. This is

dx.doi.org/10.1021/ct500422t | J. Chem. Theory Comput. 2014, 10, 3726−3737

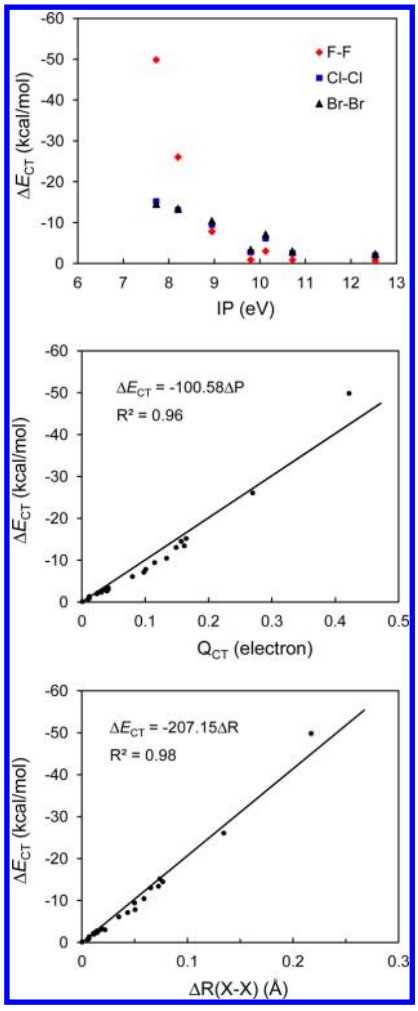

Figure 4. BLW trends: (a) ΔE_{CT} values for various $Me_nH_{3-n}N{:}\cdots X{-}X$ complexes (**1**−**21**) as a function of the ionization potential of Y:, $IP_{Y:}$, (b) ΔE_{CT} vs the amount of charge transferred to the dihalogen molecule Q_{CT}, in **1**−**24**, (c) ΔE_{CT} vs the X−X bond lengthening ΔR(X−X) in **1**−**24**.

truly the case as can be seen from the SI (R^2 = 0.91 and 0.84, respectively, SI Figures S7 and S8).

Yet another feature of CT mixing is the lengthening of the X−X bond. Thus, as the CT mixing increases, the X−X bond should elongate. Once again, as shown in Figure 4c, the charge transfer energy contribution, ΔE_{CT}, correlates very well (R^2 = 0.99) with lengthening of the X−X bond, ΔR(X−X). Furthermore, since ΔE_{CT} dominates the interaction and binding energies, ΔE_{int} and ΔE_b, the latter quantities correlate too with ΔR(X−X) (See SI Figures S3 and S4).

Finally, Figure 5 shows the electron density difference (EDD) between the regular DFT and BLW, which exhibits the electron transfer from Lewis bases to dihalogens in the five typical examples. Most of the transferred electron density comes from the central nitrogen or oxygen atom, but for the complexes of $Me_3N{\cdots}F_2$, the methyl groups lose significant electron density as well. The large amount of electron density shifted from Me_3N to F_2 effectively weakens the F−F bond whose bond distance is stretched by 0.2174 Å (also see Figure 4).

In summary, the X-bonds **1**−**24** in Scheme 1 and Table 1 are charge transfer complexes, and many of their features are shaped by the dominant ΔE_{CT} contribution. Considering the

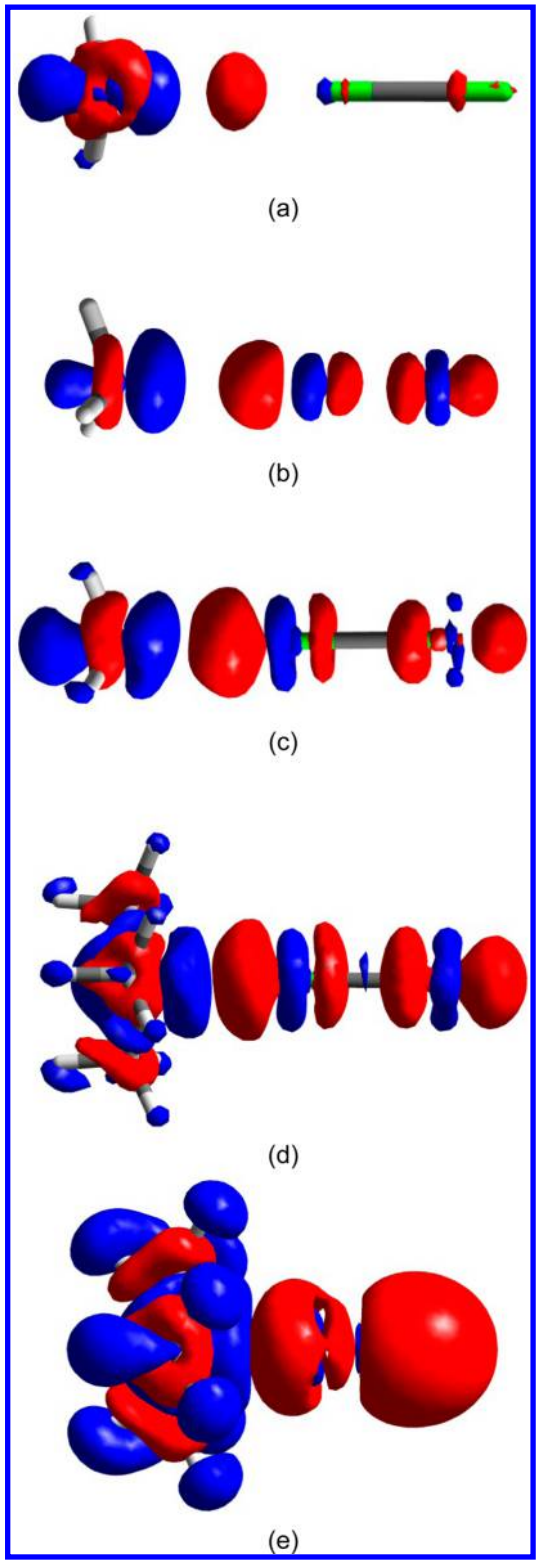

Figure 5. Electron density difference (EDD) maps showing the electron transfer in (a) $H_2O{\cdots}Cl_2$; (b) $H_3N{\cdots}F_2$; (c) $H_3N{\cdots}Cl_2$; (d) $Me_3N{\cdots}Cl_2$; (e) $Me_3N{\cdots}F_2$. The isodensity value is 0.001 au.

fact that F_2 does not possess an effective σ-hole (see SI Figure S1), while all other dihalogens do, the finding that all the complexes including those of F_2 are dominated by the CT energy is a pleasing uniformity.

Trends in the Binding Energies of X-Bonds 25−36. The H_3M−X molecules in the systems in **25**−**36** are relatively

dx.doi.org/10.1021/ct500422t | J. Chem. Theory Comput. 2014, 10, 3726−3737

weaker electron acceptors compared with dihalogens. As such, the donor−acceptor relationship of the corresponding X-bonded complexes is less pronounced than for the systems in **1**−**24**. Accordingly, the CT interactions are not expected to dominate the total binding energies as clearly as in **1**−**24**. Indeed, all energy terms make now quite comparable contributions to the interaction energies in these complexes. Since the global picture of this set of molecule is rather consistent, all the data set is relegated to the SI (Table S3), while here we present a sample of representative cases that are displayed in Figure 6.

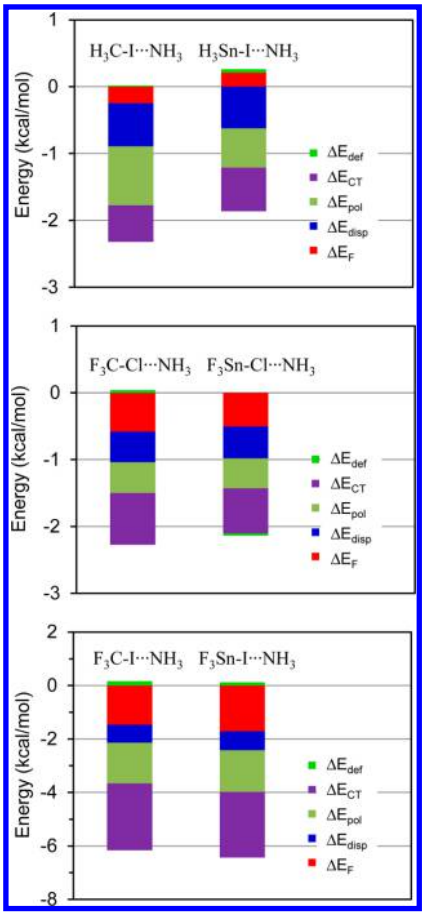

Figure 6. Representative $H_3M-X\cdots NH_3$ and $F_3M-X\cdots NH_3$ X-bonds with increasing donor−acceptor relationships, along with the various contributions to the binding energies (values in kcal mol^{-1}): (a) $H_3C-I\cdots NH_3$ and $H_3Sn-I\cdots NH_3$, (b) $F_3C-Cl\cdots NH_3$ and $F_3Sn-Cl\cdots NH_3$, and (c) $F_3C-I\cdots NH_3$ and $F_3Sn-I\cdots NH_3$.

In each part of the Figure, the H_3M-X molecules with M = C and Si are electron acceptors of comparable strength. However, as we move from parts a−c via b, the respective Z_3M-X (Z = H and F) molecules become better electron acceptors. To analyze the X-binding energies we use the terms defined in Figure 1d. In all the six cases in Figure 6, the binding energy, ΔE_b, is completely dominated by the corresponding interaction energy, ΔE_{int} (see definitions in Figure 1d), which reflects the fact that the deformation energies are negligibly small. Among the six cases, only in $H_3Sn-I\cdots NH_3$ the interaction between the molecules in the frozen Lewis state, ΔE_F, is slightly positive, which means that the electrostatic interactions do not compensate for the Pauli repulsion and cannot drive an X-bond. In the remaining five systems, however, ΔE_F, is negative and makes significant contribution to the stabilization of the complexes. The interaction energy is composed of dispersion, polarization and CT contributions. In Figure 6a and b, the three terms contribute similarly to the X-binding energy, but as we move to the best donor−acceptor pair in Figure 4c, the CT energy becomes significant (~40% of ΔE_b), and larger than both the polarization and dispersion energies. Donald et al. made a similar observation on the more extensive set of complexes, which contained also the F_3Pb-I molecule.[43] These general trends are common to the entire set. Thus, the role of polarization is not overwhelming. While the CT is not the sole driver of the interaction as in **25**−**36**, it is still a major player if not the key one. Furthermore, the CT quantity exhibits all the correlations we discussed above for **1**−**24**; it determines the amount of charge transfer ΔQ_{CT} and the M−X bond elongation. A complete correlation for all systems **1**−**36** presented in Figure S5 in SI.

Selectivity of X-Bonding in 37−55. The survey of protein and nucleic acid structures reveals that halogen bonds are abound and play an important role in ligand binding and molecular folding.[14] As such, we investigated complexes **37**−**55**, which are of biological significance, in order to discover selectivity patterns in the location of the X-bond for ambient Lewis bases. The systems in $\mathbf{37}_{\sigma,\pi}$ mimic the interactions of halogenated molecules with the simplest peptide bond as in formamide. We found that the most stable cluster has an additional hydrogen bond NH···Br (see SI Figure S6 and Table S4), apart from the in-planar X-bond. This conformation is more stable by 0.7 kcal mol^{-1} than another in-planar conformation where the NH_2 group is in the opposite direction of methyl bromide and cannot form with it a hydrogen bond. The π conformation is not a local minimum in the energy surface and was obtained by constrained optimization, with the O−Br−C angle fixed at 90°. Figure 7 shows the resulting σ and

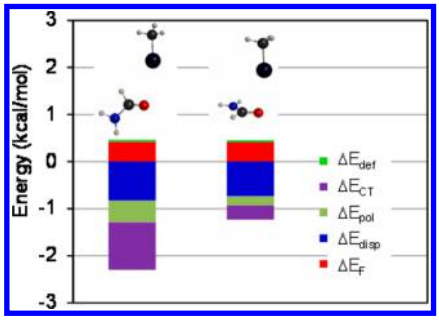

Figure 7. σ- and π-conformers $\mathbf{37}_\sigma$ and $\mathbf{37}_\pi$ along with the various contributions to the binding energies.

π conformations along with the energy contributions to the interaction energies. Much like in the $Z_3MX\cdots NH_3$ systems, here too the interaction energy is close to the binding energy as the deformation energy is negligible (less than 0.04 kcal mol^{-1}). It is seen that $\mathbf{37}_\sigma$ is slightly preferable over $\mathbf{37}_\pi$. BLW analyses show that both conformations have similar and positive ΔE_F values, indicating that the electrostatic interactions do not overcome the Pauli repulsion. Adding the dispersion contribution, the overall steric effect, however, is negative, suggesting that the van der Waals interaction can drive the complexation of formamide and methyl bromide. Both the polarization and CT interaction in the σ conformation are stronger than in the π conformation, and the CT energy in the former is comparable to the dispersion effect. Still, the

dx.doi.org/10.1021/ct500422t | J. Chem. Theory Comput. 2014, 10, 3726−3737

preference of the σ-conformer over the π-conformer is largely determined by the relative CT interactions, as Figure 7 shows.

The X-bonded complexes **38**−**55** are far more interesting in terms of selectivity and the nature of the driving force of X-bonding. These are complexes of dihalogens (X_2) with pyridine and with dimethylaminopyridine. For each dihalogen we show three types of complexes; a σ-type complex with X_2 approaching the nitrogen lone pair and forming the N···XX bond in the plane of pyridine, a π-type complex where X_2 is coordinated to the π-system and thus perpendicular to the pyridine ring, and $\sigma+\pi$ double-complexes with both N···XX and π−XX interactions. Figure 8 shows the complexes with pyridine, along with the energy contribution to the binding energy, while Figure 9 shows the complexes with dimethylaminopyridine.

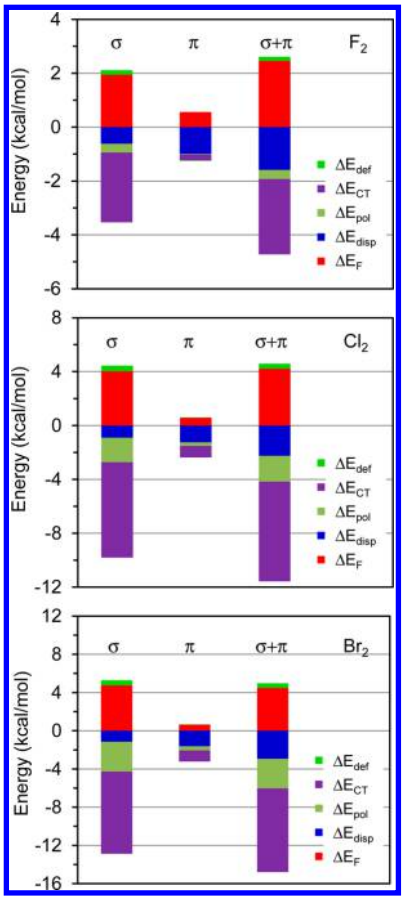

Figure 8. σ-, π-, and $\sigma+\pi$ conformers **38**−**46** of pyridine with X_2 = F_2, Cl_2, and Br_2; shown along with the various contributions to the binding energies.

A remarkable and common feature in Figures 8 and 9 is that *the binding energy and the various components behave quite additively*, such that each energy term of the $\sigma+\pi$ double-complex is given approximately as the sum of the individual contributions of the σ and π monocomplexes. This finding is reminiscent of the observation made by Voth et al. on the coexistence and orthogonality of X-bond and H-bond with peptides.[18]

Even more interestingly, is the finding that for all the 18 complexes the π monocomplex is considerably weaker than the corresponding σ monocomplex. Thus, there is a clear selectivity of the X-bond in favor of the σ monocomplex. In other words,

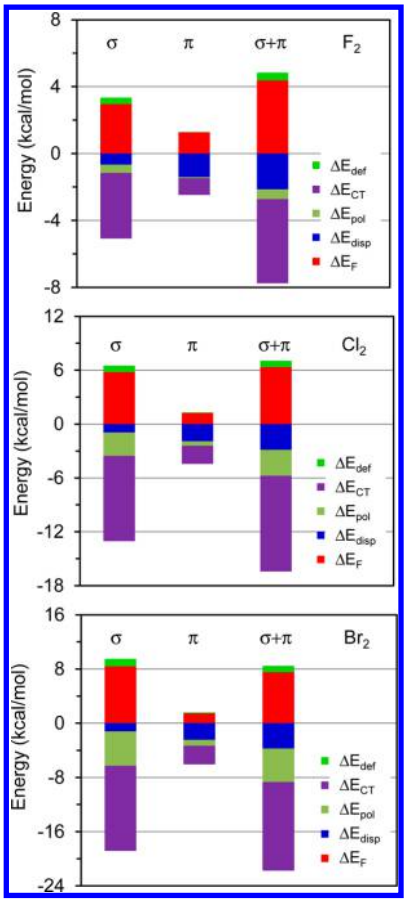

Figure 9. σ-, π- and $\sigma+\pi$ conformers **47**−**55** of dimethylaminopyridine with X_2 = F_2, Cl_2, and Br_2; shown along with the various contributions to the binding energies.

the lone nitrogen pair in the pyridine ring, which is much more basic than the π cloud, makes the stronger halogen bonds.

Furthermore, in all the nine σ complexes ΔE_F values are positive and large. Although both polarization and dispersion are stabilizing forces, the sum of ΔE_{POL} and ΔE_{Disp} is not sufficient to offset ΔE_F, suggesting that electrostatic interactions, polarization, and dispersion are not able to override the Pauli repulsion in these complexes. Indeed, the polarization energy ΔE_{POL} in all complexes accounts for a small portion of the total binding energy ΔE_b. And finally, with the exception of the π monocomplexes where the dispersion is as important as the CT energy, in all other complexes the CT energy is larger than the sum of electrostatic and Pauli repulsion energy (ΔE_F), and thus dominates the bonding energy. As such, both the total binding energies as well as the σ-selectivity of the X-bonds are driven by the CT stabilization energy.

CONCLUSIONS

This study combines the insights of a bottom-up approach based on ab initio valence bond (VB) theory, and the block-localized wave function (BLW) theory that uses monomers to reconstruct the supermolecular wave function of a complex, in order to elucidate the physical nature of the halogen bond vis-à-vis other weak intermolecular interactions. To this end, we studied the nature of 55 X-bonds in representative complexes enumerated in Scheme 1. *Our conclusion is clear-cut, most of the X-bonds are held by charge transfer interactions as envisioned more than 60 years ago by Mulliken.* This is consistent with the

experimental and computational findings that X-bonds are more directional than H-bonds. There is also a good linear correlation between charge transfer energies and total interaction energies, which implies that the important charge transfer effect can be inexplicitly incorporated into the force fields by adjusting the electrostatic energy term, that is, the partial atomic charges. The remarkable success of simple force fields in the simulation of large systems involving X-bonds endorses our findings. Furthermore, the use of the CT energy (IP-EA) to design X-bonds of desired strengths is simple and can be a productive design tool.

Whenever the X bond donor is a weak electron acceptor such as the M−X bond (M = C and Si), all terms including electrostatic, polarization, dispersion and CT, contribute to the overall bonding energy. However, even in these cases, the CT energy is a key player.

For halogen bonds in biological-like systems, our study reveals two remarkable findings concerning the selectivity of X-bonds. Thus, for example, in substituted pyridine Lewis donors, the dihalogen molecule prefers the N:···XX interaction over the π···XX interaction, and this selectivity is dominated by the strong $n \rightarrow \sigma^*_{XX}$ charge transfer (hyperconjugative) interaction. Furthermore, double-halogen complexes where both N:···XX and π−XX interactions are present exhibit a complete additivity of all the energy terms, in accord with the recent experimental evidence.[18] The architectural elements of these two X-binding sites, and the additivity of the binding and CT energies can be utilized to design 3D nanomaterials from appropriate donor−acceptor molecules (e.g, 1,4-dihalotetrafluorobenzene with pyrazines). The cohesion energies might be sufficiently strong to stabilize the assemblies.

We note that most recently, Yan et al. demonstrated and increased cooperative effects in multiple halogen bonding systems, presumably due to the polarization effect.[76] While this finding merits further analysis, we remark that the large dipole moments of interacting monomers may play a role in these multiple halogen bonding systems.

METHODS

The VB calculations were at the BOVB level using the XMVB package.[77] The basis sets used were 6-31G*, 6-311+G*, and cc-pVTZ. Our VB procedure is based on natural localized molecular orbitals (NLMO) as described in our previous work.[66] Since VB calculations are demanding, we carried out only single point calculations on the DFT optimized complexes, and limited our study to five representative complexes ($H_3N\cdots X_2$ and $Me_3N\cdots X_2$ (X = F and Cl), and $H_2O\cdots Cl_2$ in Scheme 1). Since we did not do geometry optimization, reporting of ΔE_{def} is meaningless, and since this quantity is very small anyway (see Table 1), it was kept embedded in the ΔE_F term. The VB data are collected in the SI, Tables S6−S10.

The BLW calculations were carried out with DFT, testing a variety of functionals, and benchmarking them against CCSD(T)/CBS calculations. Being aware of the possibility that these complexes may well be stabilized by CT interactions, we tested quite a few range-separated functionals,[78−80] which downsize the CT contribution. Our benchmark, led to the conclusion that ωB97x-D/cc-pVTZ[72] performs among the best functionals tried. Our usage of a higher basis set does not change the trends (SI Tables S12−S13). A similar conclusion as recently reached by Martin and Kozuch.[13] All BLW computations were performed with our in-house version of the quantum mechanical software GAMESS.[81]

The EDD and σ-hole calculations were performed with Gaussian09[82] and visualized with GaussView.[83]

ASSOCIATED CONTENT

Supporting Information

Detailed structural information and computational results and complete list for ref 79. This material is available free of charge via the Internet at http://pubs.acs.org.

AUTHOR INFORMATION

Corresponding Authors

*Email: sason@yfaat.ch.huji.ac.il.

*Email: yirong.mo@wmich.edu.

Funding

The work in HU is supported by the Indian−Israel grant, and partially by the Israel Science Foundation (ISF Grant 1183/13), and a Minerva project grant. Y.M. acknowledges the support by the U.S. National Science Foundation under Grants CHE-1055310 and CNS-1126438.

Notes

The authors declare no competing financial interest.

ABBREVIATIONS

CT, charge transfer; X-bond, halogen bond; VB, valence bond; MO, molecular orbital; BLW, block-localized wave function; POL, polarization; ES, electrostatics; DISP, dispersion; EDA, energy decomposition analysis; BOVB, breathing orbital VB; BSSE, basis set superposition error; NBO, natural bond orbital; HOMO, highest occupied MO; LUMO, lowest unoccupied MO; IP, ionization potential; EA, electron affinitiy

REFERENCES

(1) Stone, A. J. *The Theory of Intermolecular Forces*; Oxford University Press: Oxford, U.K., 2013.

(2) Arunan, E. Hydrogen Bond Seen, Halogen Bond Defined and Carbon Bond Proposed: Intermolecular Bonding, a Field That Is Maturing. *Curr. Sci.* **2013**, *105*, 892−894.

(3) Ball, P. What is a Bond? *Chemistry World* **2014**, *February*, 50−54.

(4) Alvarez, S. A Cartography of van der Waals Territories. *Dalton Trans.* **2013**, *42*, 8617−8636.

(5) Mahadevi, A. S.; Sastry, G. N. Cation−π Interaction: Its Role and Relevance in Chemistry, Biology, and Material Science. *Chem. Rev.* **2013**, *113*, 2100−2138.

(6) Schreiner, P. R.; Chernish, L. V.; Gunchenko, P. A.; Tikhonchuk, E. Y.; Hausmann, H.; Serafin, M.; Schlecht, S.; Dahl, J. E.; Carlson, R. M.; Fokin, A. A. Overcoming Liability of Extremely Long Alkane Carbon−Carbon Bonds Through Dispersionforces. *Nature* **2011**, *477*, 308−311.

(7) Desiraju, G. R.; Steiner, T. *The Weak Hydrogen Bond: In Structural Chemistry and Biology (International Union of Crystallography Monographs on Crystallography)*; Oxford University Press: New York, 2001.

(8) Jeffrey, G. A. *An Introduction to Hydrogen Bonding*; Oxford University Press: New York, 1997.

(9) Maréchal, Y. *The Hydrogen Bond and the Water Molecule: The Physics and Chemistry of Water, Aqueous and Bio-Media*; Elsevier Science: Oxford, U.K., 2007.

(10) Scheiner, S. *Hydrogen Bonding: A Theoretical Perspective*; Oxford University Press: New York, 1997.

(11) Legon, A. C. The Halogen Bond: An Interim Perspective. *Phys. Chem. Chem. Phys.* **2010**, *12*, 7736−7747.

(12) Netrangolo, P.; Resnati, G. *XB Halogen Bonding*. http://www.halogenbonding.eu (accessed May 14, 2014).

(13) Kozuch, S.; Martin, J. M. L. Halogen Bonds: Benchmarks and Theoretical Analysis. *J. Chem. Theory Comput.* **2013**, *9*, 1918−1931.
(14) Auffinger, P.; Hays, F. A.; Westhof, E.; Ho, P. S. Halogen Bonds in Biological Molecules. *Proc. Natl. Acad. Sci. U.S.A.* **2004**, *101*, 16789−16794.
(15) Hardegger, L. A.; Kuhn, B.; Spinnler, B.; Anselm, L.; Ecabert, R.; Stihle, M.; Gsell, B.; Thoma, R.; Diez, J.; Benz, J.; Plancher, J. M.; Hartmann, G.; Banner, D. W.; Haap, W.; Diederich, F. Systematic Investigation of Halogen Bonding in Protein−Ligand Interactions. *Angew. Chem., Int. Ed.* **2011**, *50*, 314−318.
(16) Parker, A. J.; Stewart, J.; Donald, K. J.; Parish, C. A. Halogen Bonding in DNA Base Pairs. *J. Am. Chem. Soc.* **2012**, *134*, 5165−5172.
(17) Manna, D.; Mugesh, G. Regioselective Deiodination of Thyroxine by Iodothyronine Deiodinase Mimics: An Unusual Mechanistic Pathway Involving Cooperative Chalcogen and Halogen Bonding. *J. Am. Chem. Soc.* **2012**, *134*, 4269−4279.
(18) Voth, A. R.; Khuu, P.; Oishi, K.; Ho, S. P. Halogen Bonds As Orthogonal Molecular Interactions to Hydrogen Bonds. *Nat. Chem.* **2009**, *1*, 74−79.
(19) Mani, D.; Arunan, E. The X-CY (X = O/F, Y = O/S/F/Cl/Br/N/P) 'Carbon Bond' and Hydrophobic Interactions. *Phys. Chem. Chem. Phys.* **2013**, *15*, 14377−14383.
(20) Mínguez Espallargas, G.; Zordan, F.; Arroyo Marín, L.; Adams, H.; Shankland, K.; van de Streek, J.; Brammer, L. Rational Modification of the Hierarchy of Intermolecular Interactions in Molecular Crystal Structures by Using Tunable Halogen Bonds. *Chem.—Eur. J.* **2009**, *15*, 7554−7568.
(21) Bertani, R.; Sgarbossa, P.; Venzo, A.; Lelj, F.; Amatic, M.; Resnati, G.; Pilati, T.; Metrangolo, P.; Terraneo, G. Halogen Bonding in Metal−Organic-Supramolecular Networks. *Coord. Chem. Rev.* **2010**, *254*, 677−695.
(22) *Valence Bond Theory*; Cooper, D. L., Ed.; Elsevier: Amsterdam, 2002.
(23) Gallup, G. A. *Valence Bond Methods: Theory and Applications*; Cambridge University Press: New York, 2002.
(24) Shaik, S. S.; Hiberty, P. C. *A Chemist's Guide to Valence Bond Theory*; Wiley: Hoboken, NJ, 2008.
(25) Wu, W.; Su, P.; Shaik, S.; Hiberty, P. C. Classical Valence Bond Approach by Modern Methods. *Chem. Rev.* **2011**, *111*, 7557−7593.
(26) Mo, Y.; Bao, P.; Gao, J. Energy Decomposition Analysis Based on a Block-Localized Wavefunction and Multistate Density Functional Theory. *Phys. Chem. Chem. Phys.* **2011**, *13*, 6760−6775.
(27) Mo, Y.; Gao, J.; Peyerimhoff, S. D. Energy Decomposition Analysis of Intermolecular Interactions Using a Block-Localized Wave Function Approach. *J. Chem. Phys.* **2000**, *112*, 5530−5538.
(28) Mo, Y.; Peyerimhoff, S. D. Theoretical Analysis of Electronic Delocalization. *J. Chem. Phys.* **1998**, *109*, 1687−1697.
(29) Mo, Y.; Song, L.; Lin, Y. The Block-Localized Wavefunction (BLW) Method at the Density Functional Theory (DFT) Level. *J. Phys. Chem. A* **2007**, *111*, 8291−8301.
(30) Guthrie, F. XXVIII.-On the Iodide of Iodammonium. *J. Chem. Soc.* **1863**, *16*, 239−244.
(31) Mulliken, R. S. Structures of Complexes Formed by Halogen Molecules with Aromatic and with Oxygenated Solvents. *J. Am. Chem. Soc.* **1950**, *72*, 600−608.
(32) Hassel, O. Structural Aspects of Interatomic Charge-Transfer Bonding. *Science* **1970**, *170*, 497−502.
(33) Dumas, J.-M.; Kern, M.; Janier-Dubry, J. L. Cryoscopic and Calorimetric Study of MX4-Polar Organic Base Interactions (M = C, SI, X = Cl, Br)—Influence of Element and of Halogen. *Bull. Soc. Chim. France* **1976**, 1785−1790.
(34) Wolters, L. P.; Schyman, P.; Pavan, M. J.; Jorgensen, W. L.; Bickelhaupt, F. M.; Kozuch, S. The Many Faces of Halogen Bonding: A Review of Theoretical Models and Methods. *WIREs Comput. Mol. Sci.* **2014**, *4*, DOI: 10.1002/wcms.1189.
(35) Clark, T. σ-Holes. *WIREs Comput. Mol. Sci.* **2013**, *3*, 13−20.
(36) Clark, T.; Hennemann, M.; Murray, J. S.; Politzer, P. Halogen Bonding: The σ-Hole. *J. Mol. Model.* **2007**, *13*, 293−296.
(37) Politzer, P.; Murray, J. S.; Clark, T. Halogen Bonding: An Electrostatically-Driven Highly Directional Noncovalent Interaction. *Phys. Chem. Chem. Phys.* **2010**, *12*, 7748−7757.
(38) Politzer, P.; Murray, J. S.; Clark, T. Halogen Bonding and Other σ-Hole Interactions: A Perspective. *Phys. Chem. Chem. Phys.* **2013**, *15*, 11178−11189.
(39) Politzer, P.; Murray, J. S. Halogen Bonding: An Interim Discussion. *ChemPhysChem* **2013**, *14*, 278−294.
(40) Wolters, L. P.; Bickelhaupt, F. M. Halogen Bonding versus Hydrogen Bonding: A Molecular Orbital Perspective. *ChemistryOPEN* **2012**, *1*, 96−105.
(41) Palusiak, M. On the Nature of Halogen Bond—The Kohn-Sham Molecular Orbital Approach. *J. Mol. Struct.: THEOCHEM* **2010**, *945*, 89−92.
(42) Stone, A. J. Are Halogen Bonds Electrostatically Driven? *J. Am. Chem. Soc.* **2013**, *135*, 7005−7009.
(43) See for example the study of 100 X-bonds: Donald, K. J.; Wittmaack, B. K.; Crigger, C. Tuning σ-Holes: Charge Redistribution in the Heavy (Group 14) Analogues of Simple and Mixed Halomethanes Can Impose Strong Propensities for Halogen Bonding. *J. Phys. Chem. A* **2010**, *114*, 7213−7222.
(44) Braida, B.; Hiberty, P. C. What Makes the Trifluoride Anion F_3^- So Special? A Breathing-Orbital Valence Bond Ab Initio Study. *J. Am. Chem. Soc.* **2004**, *126*, 14890−14898.
(45) Shaik, S. S.; Bar, R. How Important Is Resonance in Organic Species? *Nouv. J. Chim.* **1984**, *8*, 411−420.
(46) Weinhold, F.; Landis, C. *Valency and Bonding*; Cambridge University Press: Cambridge, U.K., 2005.
(47) Grabowski, S. J. Hydrogen and Halogen Bonds Are Ruled by the Same Mechanisms. *Phys. Chem. Chem. Phys.* **2013**, *15*, 7249−7259.
(48) Mo, Y.; Wang, C.; Guan, L.; Braïda, B.; Hiberty, P. C.; Wu, W. On the Nature of Blue-Shifting Hydrogen Bonds. *Chem.—Eur. J.* **2014**, *20*, 8444−8452.
(49) Danovich, D. OVGF AM1 Calculations on the Ionization Energies of Pyridine Derivatives. *J. Mol. Struct.: THEOCHEM* **1990**, *209*, 77−87.
(50) Kitaura, K.; Morokuma, K. A New Energy Decomposition Scheme for Molecular Interactions within the Hartree-Fock Approximation. *Int. J. Quantum Chem.* **1976**, *10*, 325−340.
(51) Morokuma, K. Why Do Molecules Interact? The Origin of Electron Donor−Acceptor Complexes, Hydrogen Bonding, and Proton Affinity. *Acc. Chem. Res.* **1977**, *10*, 294−300.
(52) Bagus, P. S.; Hermann, K.; Bauschlicher, C. W., Jr. A New Analysis of Charge Transfer and Polarization for Ligand−Metal Bonding: Model Studies of Carbonylaluminum (Al_4CO) and Ammineraluminum (Al_4NH_3). *J. Chem. Phys.* **1984**, *80*, 4378−4386.
(53) Chen, W.; Gordon, M. S. Energy Decomposition Analyses for Many-Body Interaction and Applications to Water Complexes. *J. Phys. Chem.* **1996**, *100*, 14316−14328.
(54) Glendening, E. D.; Streitwieser, A. Natural Energy Decomposition Analysis—An Energy Partitioning Procedure for Molecular-Interactions with Application to Weak Hydrogen-Bonding, Strong Ionic, and Moderate Donor−Acceptor Interactions. *J. Chem. Phys.* **1994**, *100*, 2900−2909.
(55) Reinhardt, P.; Piquemal, J.-P.; Savin, A. Fragment-Localized Kohn−Sham Orbitals via A Singles Configuration-Interaction Procedure and Application to Local Properties and Intermolecular Energy Decomposition Analysis. *J. Chem. Theory Comput.* **2008**, *4*, 2020−2029.
(56) Stevens, W. J.; Fink, W. H. Frozen Fragment Reduced Variational Space Analysis of Hydrogen Bonding Interactions. Application to the Water Dimer. *Chem. Phys. Lett.* **1987**, *139*, 15−22.
(57) Su, P.; Li, H. Energy Decomposition Analysis of Covalent Bonds and Intermolecular Interactions. *J. Chem. Phys.* **2009**, *131*, 014101.
(58) van der Vaart, A.; Merz, K. M., Jr. Divide and Conquer Interaction Energy Decomposition. *J. Phys. Chem. A* **1999**, *103*, 3321−3329.

(59) Wu, Q.; Ayers, P. W.; Zhang, Y. K. Density-Based Energy Decomposition Analysis for Intermolecular Interactions with Variationally Determined Intermediate State Energies. *J. Chem. Phys.* **2009**, *131*, 164112.
(60) Ziegler, T.; Rauk, A. On the Calculation of Bonding Energies by the Hartree−Fock−Slater Method. *Theor. Chem. Acc.* **1977**, *46*, 1−10.
(61) Hirao, H. Reactive Bond Orbitals: A Localized Resonance−Structure Approach to Charge Transfer. *Chem. Phys. Lett.* **2007**, *443*, 141−146.
(62) Shaik, S.; Shurki, A. Valence Bond Diagrams and Chemical Reactivity. *Angew. Chem., Int. Ed.* **1999**, *38*, 586−625.
(63) Hiberty, P. C.; Flament, J. P.; Noizet, E. Compact and Accurate Valence Bond functions with Different Orbitals for Different Configurations: Application to the Two-Configuration Description of F_2. *Chem. Phys. Lett.* **1992**, *189*, 259−265.
(64) Hiberty, P. C.; Humbel, S.; Byrman, C. P.; van Lenthe, J. H. Compact Valence Bond Functions with Breathing Orbitals: Application to the Bond Dissociation Energies of F_2 and FH. *J. Chem. Phys.* **1994**, *101*, 5969−5976.
(65) Mo, Y.; Song, L.; Wu, W.; Zhang, Q. Charge Transfer in the Electron Donor−Acceptor Complex BH_3NH_3. *J. Am. Chem. Soc.* **2004**, *126*, 3974−3982.
(66) Danovich, D.; Shaik, S.; Nesse, F.; Echeverria, J.; Aullon, G.; Alvarez, S. Understanding the Nature of the CH−HC Interactions in Alkanes. *J. Chem. Theory Comput.* **2013**, *9*, 1977−1991.
(67) Echeverria, J.; Aullon, G.; Danovich, D.; Shaik, S.; Alvarez, S. Dihydrogen Contacts in Alkanes Are Subtle But Not Faint. *Nat. Chem.* **2011**, *3*, 323−330.
(68) Bickelhaupt, F. M.; Baerends, E. J. In *Rev. Comp. Chem.*; Lipkowitz, K. B., Boyd, D. B., Eds.; Wiley-VCH: New York, 1999; Vol. *15*, p 1.
(69) Von Hopffgarten, M.; Frenking, G. Energy Decomposition Analysis. *Wires Comput. Mol. Sci.* **2012**, *2*, 43−62.
(70) Strozier, R. W.; Caramella, P.; Houk, K. N. Influence of Molecular Distortions Upon Reactivity and Stereochemistry in Nucleophilic Additions to Acetylenes. *J. Am. Chem. Soc.* **1979**, *101*, 1340−1343.
(71) Dandamudi, U.; Lacy, D. C.; Borovik, A. S.; Shaik, S. Dichotomous Hydrogen Atom Transfer vs Proton-Coupled Electron Transfer During Activation of X−H Bonds (X = C, N, O) by Nonheme Iron−Oxo Complexes of Variable Basicity. *J. Am. Chem. Soc.* **2013**, *135*, 17090−17104.
(72) Chai, J.-D.; Head-Gordon, M. Long-Range Corrected Hybrid Density Functionals with Damped Atom−Atom Dispersion Corrections. *Phys. Chem. Chem. Phys.* **2008**, *10*, 6615−6620.
(73) Grimme, S. Semiempirical GGA-type Density Functional Constructed with a Long-Range Dispersion Correction. *J. Comput. Chem.* **2006**, *27*, 1787−1799.
(74) Mo, Y.; Subramanian, G.; Gao, J.; Ferguson, D. M. Cation−π Interactions: An Energy Decomposition Analysis and Its Implication in δ-Opioid Receptor···Ligand Binding. *J. Am. Chem. Soc.* **2002**, *124*, 4832−4837.
(75) Guan, L.; Mo, Y. Electron Transfer in Pnicogen Bonds. *J. Phys. Chem. A* **2014**, DOI: 10.1021/jp500775m.
(76) Yan, X. C.; Schyman, P.; Jorgensen, W. L. Cooperative Effects and Optimal Halogen Bonding Motifs for Self-Assembling Systems. *J. Phys. Chem. A* **2014**, *118*, 2820−2826.
(77) Song, L.; Mo, Y.; Zhang, Q.; Wu, W. XMVB: A Program for Ab Initio Nonorthogonal Valence Bond Computations. *J. Comput. Chem.* **2005**, *26*, 514−521.
(78) Stein, T.; Kronik, L.; Baer, R. Reliable Prediction of Charge Transfer Excitations in Molecular Complexes Using Time-Dependent Density Functional Theory. *J. Am. Chem. Soc.* **2009**, *131*, 2818−2820.
(79) Refaely-Abramson, S.; Baer, R.; Kronik, L. Fundamental and Excitation Gaps in Molecules of Relevance for Organic Photovoltaics from Anoptimally Tuned Range-Separated Hybrid Functional. *Phys. Rev. B* **2011**, *84*, 075144.
(80) Karolewski, A.; Kronik, L.; Kümmel, S. Using Optimally Tuned Range Separated Hybrid Functionals in Ground-State Calculations: Consequences and Caveats. *J. Chem. Phys.* **2013**, *138*, 204115.
(81) Schmidt, M. W.; Baldridge, K. K.; Boatz, J. A.; Elbert, S. T.; Gordon, M. S.; Jensen, J. J.; Koseki, S.; Matsunaga, N.; Nguyen, K. A.; Su, S.; Windus, T. L.; Dupuis, M.; Montgomery, J. A. General Atomic and Molecular Electronic Structure System. *J. Comput. Chem.* **1993**, *14*, 1347−1363.
(82) Frisch, M. J.; Trucks, G. W.; Schlegel, H. B.; Scuseria, G. E.; Robb, M. A.; Cheeseman, J. R.; Scalmani, G.; Barone, V.; Mennucci, B.; Petersson, G. A.; Nakatsuji, H.; Caricato, M.; Li, X.; Hratchian, H. P.; Izmaylov, A. F.; Bloino, J.; Zheng, G.; Sonnenberg, J. L.; Hada, M.; Ehara, M.; Toyota, K.; Fukuda, R.; Hasegawa, J.; Ishida, M.; Nakajima, T.; Honda, Y.; Kitao, O.; Nakai, H.; Vreven, T.; Montgomery, J., J. A. ; Peralta, J. E.; Ogliaro, F.; Bearpark, M.; Heyd, J. J.; Brothers, E.; Kudin, K. N.; Staroverov, V. N.; Keith, T.; Kobayashi, R.; Normand, J.; Raghavachari, K.; Rendell, A.; Burant, J. C.; Iyengar, S. S.; Tomasi, J.; Cossi, M.; Rega, N.; Millam, J. M.; Klene, M.; Knox, J. E.; Cross, J. B.; Bakken, V.; Adamo, C.; Jaramillo, J.; Gomperts, R.; Stratmann, R. E.; Yazyev, O.; Austin, A. J.; Cammi, R.; Pomelli, C.; Ochterski, J. W.; Martin, R. L.; Morokuma, K.; Zakrzewski, V. G.; Voth, G. A.; Salvador, P.; Dannenberg, J. J.; Dapprich, S.; Daniels, A. D.; Farkas, O.; Foresman, J. B.; Ortiz, J. V.; Cioslowski, J.; Fox, D. J. *Gaussian09*, Revision C.01; Gaussian, Inc.: Wallingford, CT, 2010.
(83) Dennington, R.; Keith, T.; Millam, J. *GaussView*, Ver. 5; Semichem Inc.: Shawnee Mission, KS, 2009.